Effects of Thermal Contact Resistance on Film Growth Rate in a Horizontal MOCVD Reactor

Ik-Tae Im*, Nag Jung Choi
Department of Automotive Engineering, Iksan National College, 194-5 Ma-dong, Iksan, Jeollabuk-do 570-752, Korea
Masakazu Sugiyama
Department of Electronic Engineering, School of Engineering, University of Tokyo, 7-3-1 Hongo, Bunkyo-ku, Tokyo 113-8656, Japan
Yoshiyaki Nakano
Research Center for Advanced Science and Technology, University of Tokyo, 4-6-1 Komaba, Meguro-ku, Tokyo 153-8904, Japan
Yukihiro Shimogaki
Department of Materials Engineering, School of Engineering, University of Tokyo, 7-3-1 Hongo, Bunkyo-ku, Tokyo 113-8656, Japan
Byoung Ho Kim
ADCOMTECH, 78-2 Munpyoung-dong, Daeduck-gu, Daejon 306-220, Korea
Kwang-Sun Kim
School of Mechatronics Engineering, Korea University of Technology and Education, 307 Gajon-ri, Byungchon-myon, Chonan 330-708, Korea

Effects of thermal contact resistance between heater and susceptor, susceptor and graphite board in a MOCVD reactor on temperature distribution and film growth rate were analyzed. One-dimensional thermal resistance model considering thermal contact resistance and heat transfer area was made up at first to find the temperature drop at the surface of graphite board. This one-dimensional model predicted the temperature drop of 18K at the board surface. Temperature distribution of a reactor wall from the three-dimensional computational fluid dynamics analysis including the gap at the wafer position showed the temperature drop of 20K. Film growth rates of InP and GaAs were predicted using computational fluid dynamics technique with chemical reaction model. Temperature distribution from the three-dimensional heat transfer calculation was used as a thermal boundary condition to the film growth rate simulations. Temperature drop due to the thermal contact resistance affected to the GaAs film growth a little but not to the InP film growth.

Key Words : Thermal Contact Resistance, Metalorganic Chemical Vapor Deposition (MOCVD), Computational Fluid Dynamics (CFD), InP, GaAs

* Corresponding Author,
E-mail : itim@iksan.ac.kr
TEL : +82-63-850-0788; **FAX** : +82-63-850-0788
Department of Automotive Engineering, Iksan National College, 194-5 Ma-dong, Iksan, Jeollabuk-do 570-752, Korea. (Manuscript **Received** October 13, 2004; **Revised** March 18, 2005)

Nomenclature

A : Area
C_0 : Constant equal to -0.57 in Eq. (10)
C_1 : Constant equal to 6.8 with units of M_g [g/mole]
c_p : Specific heat at constant pressure

D_H : Hydraulic diameter
f : Mole fraction
g : Temperature jump distance, Eq. (9)
$\vec{g}$: Gravitational acceleration
H : Molar enthalpy
$\vec{j}_i$: Total diffusive mass flux of the i-th species
k : Heat conductivity
M : Molecular weight
m : Gas species mass fraction
P : Pressure
Pr : Prandtl number
R : Gas constant
Re : Reynolds number
R_k^g : Forward gas-phase reaction rate
R_{-k}^g : Reverse gas-phase reaction rate
r : The ratio of molecular masses of gas and solid
T : Temperature
t : Thickness
$\vec{v}$: Velocity vector

Greeks

α : The accommodation coefficient, Eq. (10)
γ : Ratio of specific heats
δ : Gap distance
ε : Emissivity
λ : Mean free path of gas molecules
μ : Viscosity of gas
v_{ik} : Stoichiometric coefficients of the i-th species in the k-th gas-phase reaction
ρ : Density of gas
σ : Stefan-Boltzmann constant

Subscripts

1 : Contact point between the heater and board
2 : Contact point between the susceptor and board
3 : Top surface of the board
b : Board
g : Gas
s : Susceptor
∞ : Bulk gas

1. Introduction

Metalorganic chemical vapor deposition (MOCVD) process of III-V materials has many advantages in the fabrication of opto-electronic devices such as good step coverage, mass production, epitaxial and selective area growth. Modeling and analysis based on the computational fluid dynamics (CFD) for MOCVD film deposition process have revealed the basic phenomena during the process (Tirtowidjojo and Pollard, 1988; Mountziaris and Jenson, 1991). Temperature control in a reactor and the wafer that is used as a substrate for film deposition is a crucial factor to get a uniform film thickness and composition. According to the study by Lum et al.(1995) in the epitaxial growth of InGaAsP/InP, As/P composition is very sensitive to wafer temperature. The photoluminescence (PL) wavelength changed to shorter wavelengths with increasing the growth temperature. The high uniformity in film thickness and composition is required for the increasing complexity of photonic integrated components and wafer size. Control of the wafer temperature uniformity becomes more and more important in modern MOCVD processes.

Since the wafer temperature profile during the film growth process is important to get uniform film in thickness and composition, the analysis on the temperature distribution in a reactor is a necessary condition for the exact film growth simulation of InP and GaAs. Authors' group has reported a series of results (Sugiyama et al., 1997, 2000; Feron et al., 2000) from systematic studies for the numerical analysis of InP and GaAs film growth by MOCVD process. For successful numerical simulations on the film growth, it is the most important thing to make a proper chemical reaction model as well as the thermal and fluid flow analysis model. We have done the kinetic study on the thermal decomposition of the source gases such as trimethylgallium (TMGa), trimethylindium (TMIn), tertiary-butylarsine (TBAs) and tertiary-butylphosphine (TBP) using a cracking reactor and Fourier transform infrared spectroscopy as a first step for making a chemical reaction model (Sugiyama et al., 1997). We have found from this experimental work that several gas species were dominant during the gas-phase reactions and finally, calculated the gas-phase reaction rate constants. Based on this experiment, the reaction model was made that TMGa,

TMIn, TBAs and TBP were decomposed as monomethylgallium (MMGa), monomethylindium (MMIn), AsH and PH, respectively. We assumed that these intermediates moved onto the substrates and formed solid films. This reaction model successfully predicted the film growth rates and compositions of GaAs (Sugiyama et al., 2000).

Though the predicted film growth rate and composition variation results were in good agreement with the experiments, the model had two obscure problems. One was the surface reaction rate constants, which were still based on the numerical analyses experience and rough theoretical estimation. To clarify the uncertainty of the numerical solutions, it was necessary to use the surface reaction rate constants obtained from well-organized experiments. The other was the difference of the growth rate profiles between InP and GaAs.

To decide the surface reaction rate constants, our group chose the wide-gap selective area growth (SAG) and reported several important experimental results (Oh et al., 2003). On the difference of the film growth mechanisms between InP and GaAs, we investigated the effects of the various control parameters such as gas-phase reaction rate constant, the surface reaction rate constant and the mass diffusivity on a film growth profile using computational fluid dynamics method (Im et al., 2004). Measured surface reaction rate data and three-dimensional heat transfer calculation were used. It was able to get reasonable numerical solutions for the film growth rate of InP and GaAs using both measured surface reaction rate and temperature from three-dimensional heat transfer calculation. Film growth characteristics were examined and limiting factors of growth rate were decided.

Through these researches, it can be said that it is still worth making an effort to obtain more accurate numerical solutions with the aid of experiments. In this study, we tried to decide where the discrepancies come from, either the reaction model including reaction rate constant or the graphite board temperature. If the exact calculation of the board temperature will not decrease the difference between the numerical solutions and experimental results, the reaction model, particularly the surface reaction rate constant for our model have to be studied intensively.

In general, temperature of the substrate where film is deposited is considered a crucial factor to the film growth rate. We concentrated on the temperature non-uniformity of the graphite board that might be caused by the thermal contact resistance between the surfaces. Temperature non-uniformity was chosen as the first research topic due to its simplicity. Study on the reaction model with surface reaction rate constant requires cost expensive experimental works due to the complexity of the phenomena. To obtain the effect of the substrate temperature profile on the InP and GaAs film growth rate, heat transfer during the process was analyzed including the thermal contact resistance between the heater and wafer susceptor, susceptor and graphite board which was set to measure the reactor scale film growth rates. A detail of the reactor structure was explained in the reference (Feron et al., 2000). One-dimensional heat flow model considering the heat transfer area was devised to evaluate thermal contact resistance effect to the temperature of the board on which the film is deposited. Full three-dimensional analyses were also carried using the commercial CFD software, FLUENT (2003) to compare the temperature distribution with one-dimensional model. Film growth rates of InP and GaAs were predicted using the three-dimensional temperature distribution and the results were compared to the previous experimental results (Feron et al., 2000).

2. Computational Model

2.1 Thermal contact resistance

Fig. 1 shows the horizontal reactor (AIXTRON AIX200/4) used in this study. The inner reactor where the reactions occur was a rectangular conduit and surrounded by a cylindrical quartz tube. The inner reactor was also made of quartz. A 267 mm-length graphite board was placed onto the bottom of the inner reactor to measure the reactor scale film growth rates. As

Fig. 1 Schematic of a horizontal MOCVD reactor

mentioned earlier, the focus of the study is to model the thermal contact resistance among the heater, susceptor and graphite board to get a precise temperature profile of the board surface where the film is deposited. Two surfaces, apparently in contact, actually touch each other only at a few individual spots, because of the microscopic and macroscopic irregularities present. Thermal contact resistance is due to the limited area of contact at such a joint. Readers interesting to the importance of thermal contact resistance in the design and operation of practical systems can refer the Madhusudana's review (Madhusudana, 1996) on thermal contact conductance.

Thermal contact resistance between the surfaces shown in Fig. 1 was considered to decide whether the surface temperature of the graphite board, used as a substrate for film growth, was affected by the contact conductance. Detail structure of the contact points and appropriate thermal flow concept are shown in Fig. 2. By using the thermal resistance concept shown in Fig. 2, board surface temperature, T_s can be written as

$$T_s=\frac{\sum R_{t,out}T_h+\sum R_{t,in}T_\infty}{\sum R_{t,in}+\sum R_{t,out}} \tag{1}$$

where

$$\sum R_{t,in}=\left(\frac{1}{R_u}+\frac{1}{R_d}\right)^{-1}+\frac{t_b}{k_sA_3} \tag{2}$$

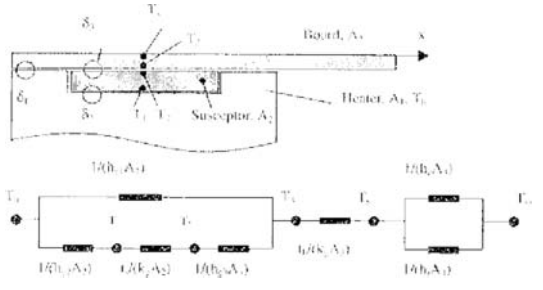

Fig. 2 Detail view on the heater, susceptor and graphite board and thermal resistance concept

Table 1 Values used to calculate the board surface temperature

Variable	Value	Unit
A_1	15896	mm^2
A_2	10936	mm^2
A_3	33375	mm^2
C_v	10120	J/kg-K
D_H	48.75	mm
M_g	2.615	g/mol
M_s	12.0	g/mol
t_b	3	mm
t_s	4	mm
γ	1.41	-

$$\sum R_{t,out}=(h_cA_3+h_rA_3)^{-1}. \tag{3}$$

R_u and R_d shown in the above equation are written as

$$R_u=\frac{1}{h_{g1}A_1} \tag{4}$$

$$R_d=\frac{1}{h_{g2}A_2}+\frac{t_s}{k_sA_2}+\frac{1}{h_{g3}A_2} \tag{5}$$

Convective and linearized radiative heat transfer coefficient at the board surface, h_c and h_r were calculated from the following equations (White, 1991 ; Özisik, 1991)

$$\frac{h_cD_H}{k_g}=2G(\mathrm{Pr})\,\mathrm{Re}^{1/2} \tag{6}$$

$$h_r=\varepsilon\sigma(T_1+T_2)(T_1^2+T_2^2) \tag{7}$$

Table 1 lists the values used in the calculations.

Heat conduction through the contact area between heater and susceptor can be modeled by the contact conduction coefficient h_{g1} that is applicable to low pressure,

$$h_{g1}=\frac{k_g}{\delta_1+g_1+g_2} \tag{8}$$

where g_1 and g_2 are the temperature jump distance for the two contact surfaces. The expression for the temperature jump distance given by Madhusudana (1996),

$$g=\frac{2-\alpha}{\alpha}\frac{2}{\gamma+1}\frac{k_g}{\mu C_v}\lambda \tag{9}$$

was used in this study. Where α, the accommodation coefficient was given as ;

Table 2 Lennard-Jones parameters used in the computation, ε/k is the potential well depths and σ is the collision diameters, respectively, where k is the Boltzmann constant

species	ε/k (K)	σ (Å)
TMGa	378	5.52
MMGa	972	4.92
TMIn	454	5.62
MMIn	1049	5.02
TBAs	397	5.98
AsH	200	4.22
TBP	376	5.93
PH	190	4.07
C_4H_8	357	5.18
CH_4	141	3.75
H_2	38	2.92

$$\alpha=\exp(C_0T)\left[\frac{M_g}{C_1+M_g}+\{1-\exp(C_0T)\}\left\{\frac{2.4\gamma}{(1+\gamma)^2}\right\}\right] \quad (10)$$

with normalized temperature, $T=(T_s-T_0)/T_0$. Expressions for h_{g2} and h_{g3} can be written as similar to the equation (8). Thermal conductivity and viscosity of the hydrogen carrier gas were calculated from the kinetic theory (Kleijn, 1994). The Lennard-Jones parameters, σ and ε/k_B of hydrogen gas were listed in Table 2 with those of other gas species used to the film growth simulations. Iteration is needed to get T_s because the properties and board surface temperature are correlated.

2.2 Computational fluid dynamics analysis

A thin graphite board instead of a wafer was used to measure the film growth rates in the experiments. There was a relatively large gap between the susceptor and graphite board shown as in Fig. 1. CFD method was used to estimate the effect of the gap depicted as δ_3 in Fig. 2 to the temperature distribution in the reactor.

Governing equations for the flow and heat transfer in the reactor were continuity equation, momentum and energy conservation equations shown in the equation (11) to (13) if the flow was assumed to be compressible, laminar and steady state.

$$\nabla\cdot(\rho\vec{v})=0 \quad (11)$$

$$\nabla\cdot(\rho\vec{v}\vec{v})=\rho\vec{g}-\nabla P+\frac{\partial}{\partial x_j}\left[\mu\left(\frac{\partial v_i}{\partial x_j}+\frac{\partial v_j}{\partial x_i}\right)-\frac{2}{3}\mu(\nabla\cdot\vec{v})\right] \quad (12)$$

$$c_p\nabla\cdot(\rho\vec{v}T)=\nabla\cdot(k_g\nabla T)+\nabla\left(RT\sum_{i=1}^{N}\frac{D_i^T}{m_i}\nabla(\ln f_i)-q_{ri}\right)+\sum_{i=1}^{N}\frac{H_i}{m_i}\nabla\cdot\vec{j}_i-\sum_{i=1}^{N}\sum_{k=1}^{K}H_i v_{ik}(R_k^g-R_{-k}^g) \quad (13)$$

Gas mixture in the reactor was assumed to obey the ideal gas law. One of the source terms in the energy equation, net radiative heat flux, q_r was calculated from the discrete transfer radiation model (DTRM) that used ray-tracing method.

The balance equation for the i-th gas species in terms of mass fractions, could be written as

$$\nabla\cdot(\rho\vec{v}\omega_i)=-\nabla\cdot\vec{j}_i+m_i\sum_{k=1}^{K}v_{ik}(R_k^g-R_{-k}^g) \quad (14)$$

Here the total diffusive mass flux of the i-th species $\vec{j}_i$ was composed of diffusion fluxes and thermal diffusion. Details on the diffusive flux can be found in the literature (Kleijn, 1994).

Detailed three-dimensional simulation of the heat transfer inside the outer quartz tube was executed. Heat transfer coefficient for the reactor outer tube wall was set to 7.5 W/m-K that was given in the reference for the similar reactor (Mucciato and Lovergine, 2000). For the simulations of the film growth, we modeled only the inner tube with the temperature profile of both the inner tube wall and the graphite board exported from the heat transfer simulation including the outer tube. Mass fractions and velocity at inlet were calculated from the mass flow rates and the assumption that the species mole fraction was proportional to the precursor partial pressure. Film deposition mechanisms and reaction chemistry used in this study were the same as those of the previous numerical study (Im et al., 2004). Table 3 shows the reaction model for the film growth of InP and GaAs. Gas-phase reactions consist of the decomposition of four source gases. This is an approximation based on the fact that source gases are dilute in our condition. The intermediates resulted from the gas-phase decomposition move onto the surface and form solid films according to two surface reactions in Table 3. Viscosity, heat conductivity and

Table 3 Chemistry reaction model used in the numerical model

gas-phase reactions			A (1/s)	Ea (kJ/mol)
$TMIn+H_2$	→	$MMIn+2CH_4$	1.86E15	186
$TMGa+H_2$	→	$MMGa+2CH_4$	2.1E14	196
TBAs	→	$AsH+C_4H_8+H_2$	5.32E15	203
TBP	→	$PH+C_4H_8+H_2$	4.42E14	219
surface reactions			A (m/s)	Ea (kJ/mol)
$MMIn+PH$	→	$InP\langle s\rangle+CH_4$	5E5	80
$MMGa+AsH$	→	$GaAs\langle s\rangle+CH_4$	1.23E9	130

mass diffusivity of each gas species were calculated from the kinetic theory using the Chapman-Enskog formula (Poling et al., 2001). Required Lennard-Jones parameters are listed in Table 2. Governing equations were solved using the commercial CFD software, FLUENT (2003) based on the finite volume method. The number of control volumes for the inner reactor was about 240 thousands and second order upwind scheme was used for discretization of the convective terms.

3. Results and Discussions

3.1 Temperature distribution

To verify the one-dimensional heat flow model explained in the section 2.1, the surface temperature of the copper plate was measured using another vertical reactor which is suitable for temperature measurement. The copper plate with the aluminum susceptor was set in the stainless steel reactor before the measurement. Electric heater was placed directly under the susceptor and hydrogen gas was injected from the top ceiling. Fig. 3 shows the measured surface temperatures and calculated ones using thermal resistance concept shown in equation (1). Symbols are measured ones and lines are calculated curves. Several values of the gap distance were tested in the calculations because no exact data were available. 10 μm gave the best-fit results to the experiment for three different pressure conditions. The one-dimensional model accurately predicted the temperature drop due to the contact resistance if the appropriate gap distance was given. According to Shimizu et al.(2004), the average gap between

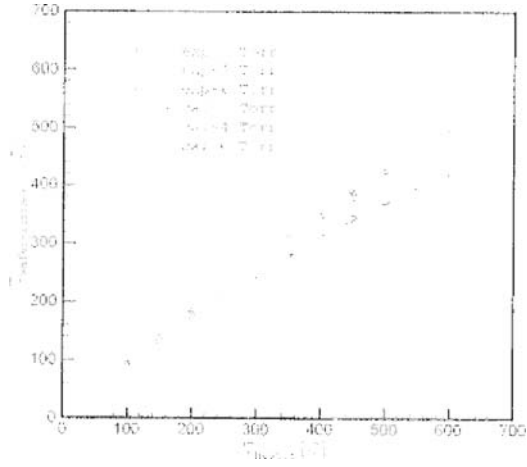

Fig. 3 Measured and calculated wafer surface temperatures in a vertical reactor at various operating pressures. The gap distance between a wafer and a susceptor was set to 10 μm in the calculations

a InP wafer and a wafer carrier was 100 μm in a vertical MOVPE reactor. From Fig. 3 and Shimizu et al.(2004), the order of the gap distance in contacts was assumed about 10 to 100 μm in this study.

Contact condition at the heater and board, δ_1 and the heater and susceptor, δ_2 were similar, but the gap at the wafer position, δ_3 was larger than δ_1 or δ_2 as shown in Fig. 2. Fig. 4 shows the board surface temperature variations when $\delta_1=\delta_2=100$ μm and $\delta_1=\delta_2=10$ μm. The gap at the wafer position, δ_3 was fixed as 1 mm. Temperature drop of 100 μm case is larger than 10 μm case since thermal contact resistance is proportional to gap size. It is noteworthy that temperature drop, ΔT becomes large when heater temperature

goes high. In the case of 100 μm, ΔT is about 14K, 18K and 23K when T_h is 773K, 883K and 973K, respectively. This increasing ΔT according to increasing T_h is mainly due to the radiation heat loss because its effect becomes dominant at high temperature as shown in equation (7). We obtained the same tendency of ΔT when the radiation heat loss term was omitted in equation (3) though its magnitude was decreased. It did not seem to be a simple problem because temperature jump distance g and gas thermal conductivity k_g were both the functions of temperature. Rigorous analysis of the magnitude for each term of the analysis results showed that the ratio of the temperature jump distance change was greater than the rate of gas thermal conductivity change. The large temperature jump distance makes the ΔT large since it acts as a thermal resistance.

Fig. 5 shows the board surface temperature according to the variations of δ_1 and δ_2 when T_h equals to 883K. As δ_1 and δ_2 increase, temperature at the board surface decreases but the relation is not proportional. Let the gap between the heater and graphite board is 100 μm, the board surface temperature is 865K and ΔT is about 18K.

Fig. 6 shows temperature profile along the centerline (x-axis) of the bottom wall of the inner liner obtained from the three-dimensional CFD simulation. Figure shows two different cases, with wafer gap depicted as a solid line, and without wafer gap depicted as a dashed line. It can be seen that the temperature decreases about 20K at the wafer position due to the wafer gap. Results from the two different methods, one-dimensional heat conduction and three-dimensional CFD method, show similar temperature drop though there is a little difference quantitatively. The three-dimensional simulations neglect the contact thermal resistance at δ_1 and δ_2. This is thought to be the main reason for the difference.

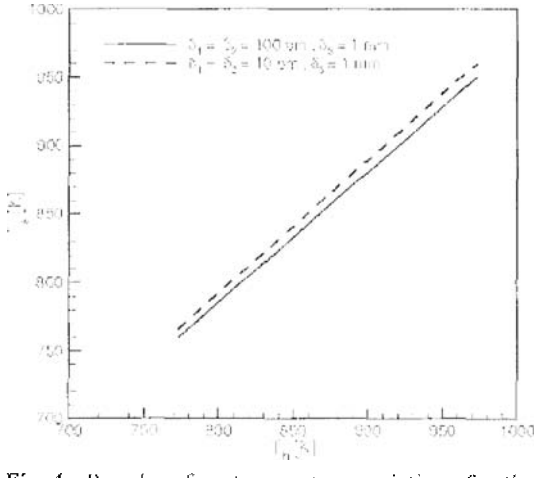

Fig. 4 Board surface temperature variations for the two different gap distances

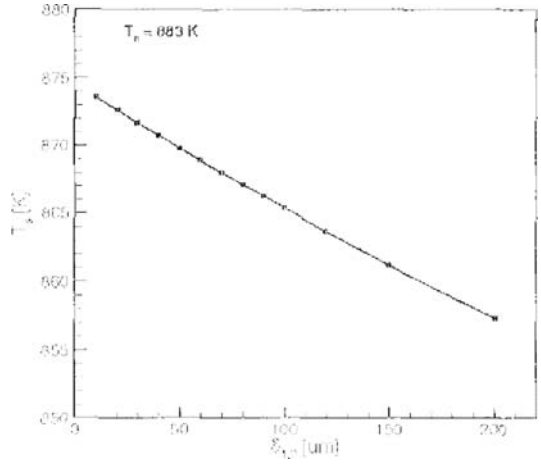

Fig. 5 Temperature variation along the board surface according to the gap distances δ_1 and δ_2 at heater temperature of 883K

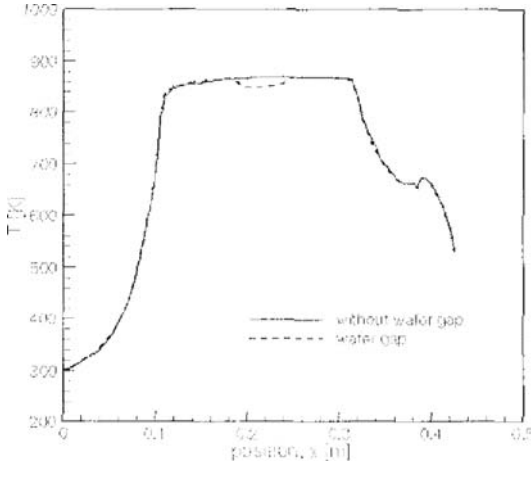

Fig. 6 Temperature profile on the symmetric plane surface of the graphite plate on which substrate were placed

3.2 Film growth rate

Film growth rates of InP and GaAs were simulated to find the effect of temperature drop due to the gap using temperature distribution from three-dimensional heat transfer calculation. TMIn, TMGa, TBAs and TBP were used as group III and group V precursors. Hydrogen gas was used as a carrier gas. Total flow rate of gas mixture was 13000 sccm and operating pressure was maintained at 10 kPa. The precursors' inlet partial pressures were 0.437, 0.573, 18 and 18 Pa for TMIn, TMGa, TBP and TBAs, respectively. The heater temperature and gas inlet temperature were assumed to be 883K and 300K, respectively. Gas inlet velocities for the upper, lower and cooling gas inlets were 1.7 m/s, 1.25 m/s and 18 m/s, which were determined from the mass flow rate, area of the inlets, pressure and temperature.

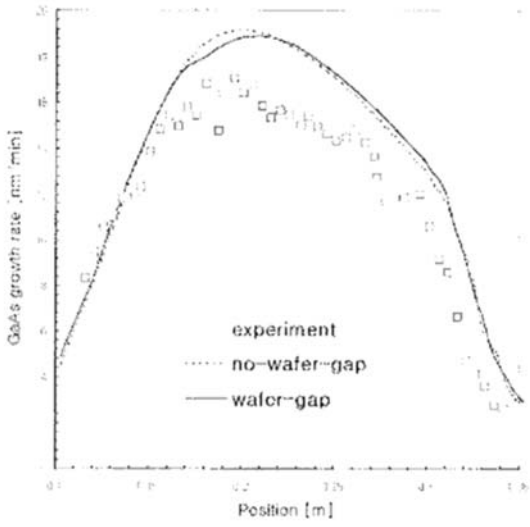

Fig. 7 Experimental data and simulated film growth rate profiles of the GaAs

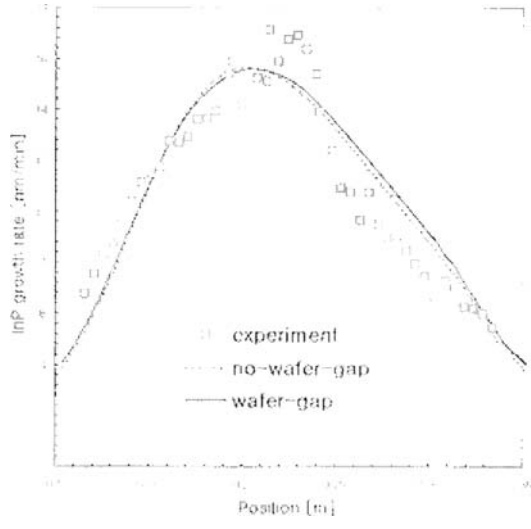

Fig. 8 Experimental data and simulated film growth rate profiles of the InP

Figs. 7 and 8 show the simulated film growth rates of GaAs and InP with experimental results for comparison. Dashed and solid lines are the simulated results with and without wafer gap. Symbols are the experimental results. Both of the simulated results agree to the experimental result in quantitatively and qualitatively. The difference between the two cases, with and without wafer gap, is hardly to differentiate in InP film growth. But it can be seen that the temperature drop of about 20K affects a little to the film growth rate at the wafer position in GaAs film growth results. It is revealed in the previous study (Im et al., 2004) that GaAs film growth is more sensitive to the temperature than InP due to the growth mechanism. The difference between the experimental result and predicted one considering temperature non-uniformity from x=0.2 to x=0.3 in Fig. 7 does not change significantly compared to the dashed 'no wafer-gap' result. Though the temperature drop affects GaAs film growth rate, it is not so large that temperature non-uniformity is important in the GaAs film growth analysis.

4. Conclusions

The effect of thermal contact resistance to the temperature distribution and resulting GaAs and InP film growth rate profile during a MOCVD process was studied by using one-dimensional heat conduction model and three-dimensional CFD calculations. One-dimensional heat conduction analyses considering thermal contact resistance gave the temperature drop of 18K at the wafer gap position. Three-dimensional CFD calculation results showed that the temperature drop was about 20K at the wafer position in the case when the gap was included. Film growth rate of

GaAs and InP were also calculated using the three-dimensional temperature simulation results as boundary conditions for inner reactor. The temperature drop changed the film growth profile of GaAs a little but did not for InP. Examination about one of the two check problems of our numerical model, temperature distribution on the reactor walls, was finished through this work. It did not seem to be that the disagreement between the experiment and numerical results, particularly at the wafer position, came from the temperature boundary condition. We have to examine and refine the reaction model further for the next step to diminish the discrepancy.

References

FLUENT is a Product of Fluent Inc., 2003, 10, Cavendish Court, Lebanon, NH, USA.

Feron, O., Sugiyama, M., Aswamethapant, W., Futakuchi, N., Feurprier, Y., Nakano, Y. and Shimogaki, Y., 2000, "MOCVD of InGaAsP, InGaAs, InGaP over InP and GaAs Substrates : Distribution of Composition and Growth rate in a Horizontal Reactor," *Appl. Surf. Sci.*, Vol. 159-160, pp. 318~327.

Im, I.-T., Oh, H. J., Sugiyama, M., Nakano, Y. and Shimogaki, Y., 2004, "Fundamental Kinetics Determining Growth Rate Profiles of InP and GaAs in MOCVD with Horizontal Reactor," *J. of Crystal Growth*, Vol. 261, pp. 214~224.

Kleijn, C. R., 1994, Chap. 4 in Computational Modeling in Semiconductor Processing, Meyyappan, M. ed., Artech House, Boston.

Lum, R. M., Mcdonald, M. L., Mack, E. M., Williams, M. D., Storez, F. G. and Levkoff, J., 1995, "Effect of Temperature on InGaAsP Alloy Composition," *J. of Electronic Materials*, Vol. 24, No. 11, pp. 1577~1581.

Madhusudana, C. V., 1996, Thermal Contact Resistance, Chap. 4, Springer-Verlag, New York.

Mountziaris, T. J. and Jenson, K. F., 1991, "Gas-phase and Surface Reaction Mechanisms in MOCVD of GaAs with Trimethylgallium and Arsine," *J. of the Electrochemical Society*, Vol. 138, No. 8, pp. 2426~2438.

Mucciato, R. and Lovergine, N., 2000, "Detailed Thermal Boundary Conditions in the 3D Fluid-dynamics Modelling of Horizontal MOVPE Reactors," *J. of Crystal Growth*, Vol. 221, pp. 758~764.

Oh, H. J., Sugiyama, M., Nakano, Y. and Shimogaki, Y., 2003, "Comparison of Organic and Hydride Group V Precursors in Terms of Surface Kinetics in Wide-gap Selective Area Metalorganic Vapor Phase Epitaxy," *Jpn. J. Appl. Phys.*, Vol. 42, pp. L1195~L1197.

Oh, H. J., Sugiyama, M., Nakano, Y. and Shimogaki, Y., 2003, "Surface reaction kinetics in metalorganic vapor phase epitaxy of GaAs through analyses of growth rate profile in wide-gap selective-area growth," *Jpn. J. Appl. Phys.*, Vol. 42, pp. 6284~6291.

Özisik, M. N., 1991, Heat Transfer, A Basic Approach, Chap. 1, McGraw-Hill, New York.

Poling, B. E., Prausnitz, J. M., O'connell, J. P., 2001, The Properties of gases and liquids, p. 9.4, McGraw-Hill, Boston.

Shimizu, E., Sugawara, S. and Nakata, H., 2004, "Computational Analysis of Wafer Temperature Non-uniformity in MOVPE System," *J. of Crystal Growth*, Vol. 266, pp. 340~346.

Sugiyama, M., Kusunoki, K., Shimogaki, Y., Sudo, S., Nakano, Y., Nagamoto, H., Sugawara, K., Tada, K. and Komiyama, H., 1997, "Kinetic Studies on Thermal Decomposition of MOVPE Sources Using Fourier Transform infrared Spectroscopy," *Applied Surface Science*, Vol. 117/118, pp. 746~752.

Sugiyama, M., Feron, O., Sudo, S., Nakano, Y., Tada, K., Komiyama, H. and Shimogaki, Y., 2000, "Kinetics of GaAs Metalorganic Chemical Vapor Deposition Studied by Numerical Analysis based on Experimental Reaction Data," *Jppn. J. Appl. Phys. Part 1*, No. 4A, Vol. 39, pp. 1642~1649.

Tirtowidjojo, M. and Pollard, R., 1988, "Elementary Processes and Rate-limiting Factors in MOVPE of GaAs," *J. of Crystal Growth*, Vol. 93, No. 1-4, pp. 108~114.

White, F. M., 1991, Viscous Fluid Flow, 2nd ed., Chap. 3, McGraw-Hill, New York.